Materials Science-Poland, 38(1), 2020, pp. 159-164
http://www.materialsscience.pwr.wroc.pl/
DOI: 10.2478/msp-2020-0018

Microstructure, transmittance and upconversion luminescence of Y_2O_3:Er^{3+} translucent ceramics

YANYAN GUO[1], XINGHUA WU[2], QINGKAI WANG[2], DIANYUAN WANG[2,*]

[1]Faculty of Mechanical and Materials Engineering, Jiujiang University, Jiujiang 332005, PR China
[2]College of Science, Jiujiang University, Jiujiang 332005, PR China

Y_2O_3:Er^{3+} translucent ceramics was fabricated with addition of $La(OH)_3$ nanopowder as a sintering aid. The influence of $La(OH)_3$ addition on the microstructure, transmittance and upconversion luminescence of Y_2O_3:Er^{3+} ceramics was investigated in detail. The results show that the ceramics sample with 5 mol % $La(OH)_3$ additives exhibits finer microstructure with fewer pores and higher optical transmittance than others. It was proved that $La(OH)_3$ additives could greatly reduce the porosity and improve the transparency of Y_2O_3:Er^{3+} ceramics. By using a 980 nm diode laser as a pumping source, the Y_2O_3:Er^{3+} ceramics gave bright visible upconversion luminescence, which was ascribed to the radiative transitions of $^2H_{11/2}$,$^4S_{3/2} \rightarrow {}^4I_{15/2}$ and $^4F_{9/2} \rightarrow {}^4I_{15/2}$ of Er^{3+} ions, respectively. The possible upconversion mechanism has been proposed accordingly.

Keywords: *ceramics; Y_2O_3; microstructure; upconversion luminescence*

1. Introduction

Y_2O_3 transparent ceramics have attracted much attention due to its applications in upconversion lasers, hypersonic guided-missile windows and domes in recent years, because it has high thermal conductivity (13.6 W/m·K), good chemical durability, thermal stability, wide spectral transparency range (0.23 – 8 μm), low laser-induced damage threshold, and relatively low phonon energy (~377 cm^{-1}) [1, 2]. However, it is difficult to grow high optical quality Y_2O_3 single-crystal because of its high melting point (~2430 °C) and structural phase transition (between cubic crystal and hexagonal crystal) in the neighborhood of 2280 °C [3, 4]. Fortunately, Y_2O_3 transparent ceramics has been successfully fabricated by using nanopowder sintering method in vacuum or H_2 atmosphere, and CW laser output has been obtained in Nd^{3+}:$Y_{1.8}La_{0.2}O_3$ and Yb^{3+}:$Y_{1.8}La_{0.2}O_3$ transparent ceramics [5, 6].

In the meantime, Er^{3+} doped Y_2O_3 ceramics has gained extensive applications in upconversion and laser emission. Er^{3+} ions have the ability to convert infrared radiation into visible light, and show potential applications in upconversion lasers and fiber optical amplifiers. Moreover, $^4I_{13/2} \rightarrow {}^4I_{15/2}$ transition of Er^{3+} ions at 1.54 μm is corresponding to atmospheric transparency and eye safety range, which makes it an excellent material widely used in communication and medical fields [7–12].

YOF crystallizes in a rhombohedral structure with space group R3m (166) [13, 14]. Because of their good physical and chemical stability and low phonon energy, YOF has been intensely investigated as matrices in upconversion luminescence [15–19]. At elevated temperatures, YOF could be converted into Y_2O_3 through heat treatment [20, 21]. In previous studies, we successfully fabricated Y_2O_3:Tm^{3+},Yb^{3+} translucent ceramics with few pores using YOF: Tm^{3+},Yb^{3+} micropowders in air atmosphere at lower sintering temperature [22], which confirmed that YOF powder proved to be a good raw material in the preparation of Y_2O_3 ceramics. In addition, $La(OH)_3$ has been used as addition to improve the densification and optical transmittance of the transparent Y_2O_3 ceramics [23].

*E-mail: 1064532@163.com

In the present work, stable $La(OH)_3$ nanopowders were introduced as La_2O_3 sources in the preparation of Y_2O_3 ceramics. The influence of $La(OH)_3$ additive on the microstructure, transmittance and upconversion luminescence of Y_2O_3:Er^{3+} ceramics was investigated using X-ray diffraction (XRD), scanning electron microscopy (SEM), transmittance spectra and photoluminescence.

2. Experimental

2.1. Preparation of YF_3:Er^{3+} and YOF:Er^{3+} nanopowders

YF_3:0.1mol%Er^{3+} nanopowders were prepared by the co-precipitation method. Y_2O_3 (4 N), Er_2O_3 (3.5 N) and NH_4F (AR) were employed as basic starting materials. RE_2O_3 (RE = Y, Er) were dissolved in dilute HNO_3 under heating to prepare the $RE(NO_3)_3$ stock solution. $Y(NO_3)_3$, $Er(NO_3)_3$ aqueous solutions and PEG200 were dispensed in deionized water and magnetically stirred. Then, NH_4F aqueous solution was added to the solution. The above solution was vigorously stirred for 1 h at 50 °C and then cooled down slowly to room temperature. Subsequently, the suspension was centrifuged, washed and dried. The product was annealed at 600 °C for 2 h and YF_3:1%Er^{3+} powders were obtained. The YOF:1%Er^{3+} nanopowders were obtained by annealing the as-prepared YF_3:1%Er^{3+} powders at 1000 °C for 3 h in air atmosphere.

2.2. Preparation of $La(OH)_3$ nanopowders

$La(NO_3)_3 \cdot 6H_2O$ (3N) and urea (AR) were used as the starting materials. In a typical procedure, $La(NO_3)_3 \cdot 6H_2O$, PEG200 and urea were added into deionized water and magnetically stirred to form a mixed solution. Then, the above solution was vigorously stirred for 2 h at 90 °C and then cooled down to room temperature. Subsequently, the suspension was centrifuged, washed and dried at 120 °C for 24 h. Finally, the resultant product was calcined at 750 °C for 2 h, and the $La(OH)_3$ nanopowders were obtained.

2.3. Fabrication of Y_2O_3:Er^{3+} translucent ceramics

The as-prepared YOF:1%Er^{3+} and $La(OH)_3$ powders were used as raw materials. The concentration of $La(OH)_3$ was 2 mol%, 5 mol% and 10 mol% in YOF:1%Er^{3+}. The raw powders of YOF:1%Er^{3+} and $La(OH)_3$ were mixed in ethanol and milled for 30 min. After that, the milled slurry was dried at 120 °C for 24 h and calcined at 600 °C for 2 h, the prepared powders were pressed into pellets with 0.5 mm thickness at 60 MPa for 10 min. The as-obtained green bodies were sintered at 1100 °C, 1300 °C and 1650 °C for 10 h, respectively.

2.4. Characterization

The crystalline structure was identified using an X-ray diffractometer (SHIMADZU XD-D1, Rigaku, Japan) with CuKα-radiation ($\lambda = 0.15418$ nm) in the range of $2\theta = 20 - 90°$. The morphology of the powders, microstructure and elemental analysis of the ceramics were studied by a scanning electron microscope and energy dispersive spectrometer (EDS) (VEGA II LSU, Tescan, Czech Republic). The transmittance spectra of unpolished ceramics were measured using a UV/VIS/NIR spectrophotometer (UV1901PC, Aucy, China) over a range of 0.3 – 1.1 μm. The upconversion emission spectra were measured and analyzed using a fluorescence spectrometer (F-4500, Hitachi, Japan) under 980 nm laser diode (LD) (Newport, USA) excitation at room temperature.

3. Results and discussion

Fig. 1 illustrates the XRD patterns of the as-prepared YF_3:Er, YOF:Er, $La(OH)_3$ powders and the fabricated Y_2O_3:Er ceramics doped with 10 mol% of $La(OH)_3$ as sintering aid. It could be seen that the patterns are basically consistent with the YF_3 phase (JCPDS 74-0911), YOF phase (JCPDS 71-2100), $La(OH)_3$ phase (JCPDS 36-1481) and cubic Y_2O_3 phase (JCPDS 25-1200), respectively. The XRD results also reveal that YF_3:Er was oxidized to YOF:Er during the annealing at

1000 °C, and that YOF:Er was completely changed to Y_2O_3:Er during the sintering process of the ceramics [22]. In addition, no other impurities were observed in the Y_2O_3:Er ceramics sample, which indicates that $La(OH)_3$ decomposed completely to La_2O_3 at elevated temperatures [23] and La^{3+} ions were doped into Y_2O_3 lattice by replacing Y^{3+} ions [11, 12].

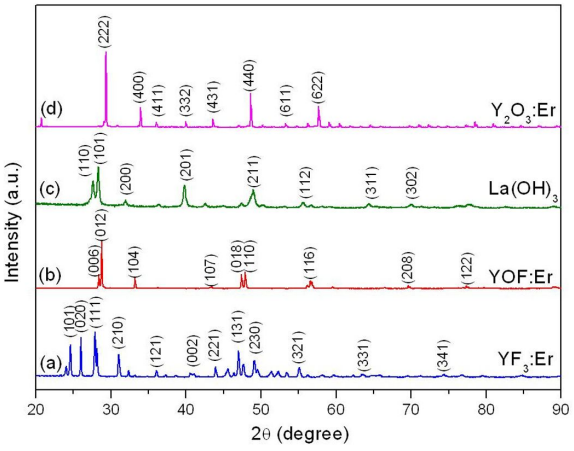

Fig. 1. XRD patterns of as-prepared YF_3:Er, YOF:Er, $La(OH)_3$ powders and the fabricated Y_2O_3:Er ceramics doped with 10 mol% of $La(OH)_3$.

Fig. 2 shows SEM images of the as-prepared YF_3:Er, YOF:Er and $La(OH)_3$ powders. It can be observed that the YF_3:Er powders shown in Fig. 2a have a round shape, good dispersion and the average particle size of 150 nm. Fig. 2b shows the morphology of the YOF:Er powders prepared by annealing with YF_3:Er powders; it can be noticed that the YOF:Er particles with smooth surface have the sizes of 400 – 800 nm, which indicates that annealing treatment leads to the growth of particles along with enhanced crystallization. The as-prepared $La(OH)_3$ powders with an average particle size of 50 nm are highly uniform and nearly spherical as shown in Fig. 2c.

The detailed microstructure and elemental composition of the as-fabricated Y_2O_3:Er ceramics were further investigated using SEM and EDS. Fig. 3 shows the SEM micrographs of the fracture surface of the Y_2O_3:Er ceramics doped with different doping concentration of $La(OH)_3$ additives. It can be observed in Fig. 3a and Fig. 3c that there

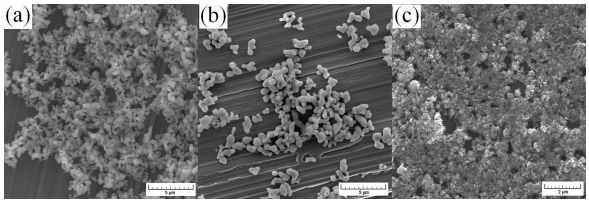

Fig. 2. SEM images of the as-prepared YF_3:Er, YOF:Er and $La(OH)_3$ powders.

are more pores in the samples doped with 2 mol% and 10 mol% $La(OH)_3$, and fewer pores on the fracture surface of the sample doped with 5 mol% $La(OH)_3$ as shown in Fig. 3b. The reason for the results mentioned above is that the decomposition of $La(OH)_3$ accelerated the material transport leading to rapid densification. The decomposition products of La_2O_3 could effectively inhibit excessive grain growth of Y_2O_3 ceramics, but when the amount of $La(OH)_3$ was higher than 5 mol%, more decomposition products such as H_2O had been remained in the ceramics and more pores were formed [23]. Fig. 4 shows that the corresponding elemental composition confirmed by EDS included Y, O, Er and La, approving the presence of Er and La elements in the Y_2O_3 ceramics sample. No F element has been found, it is because the YOF was sintered in air and completely transformed into Y_2O_3.

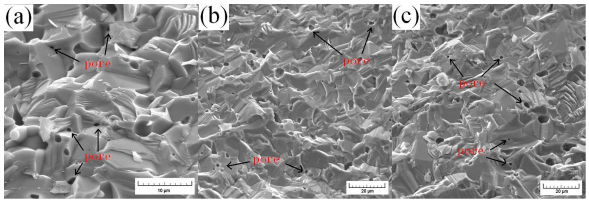

Fig. 3. Fracture surface of the Y_2O_3:Er ceramics doped with (a) 2 mol% $La(OH)_3$, (b) 5 mol% $La(OH)_3$, (c) 10 mol% $La(OH)_3$.

Fig. 5 shows the photographs of the unpolished Y_2O_3:Er ceramics samples sintered at 1650 °C for 10 h after annealing at 1100 °C and 1300 °C for 10 h, respectively. All the samples exhibit good transparency. Words behind them can be read. As can be seen from the optical transmittance spectra of the unpolished Y_2O_3:Er ceramics samples shown in Fig. 6, the optical values of transmittance

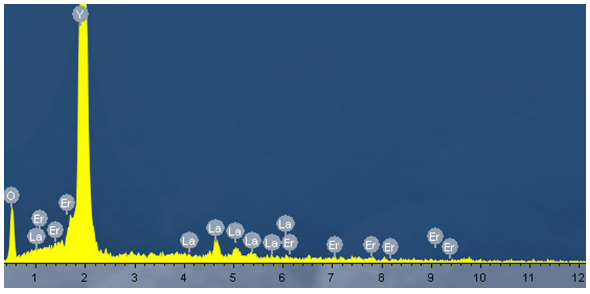

Fig. 4. EDS spectrum of the Y_2O_3:Er ceramics doped with 5 mol% $La(OH)_3$.

are all above 0.6 % at 1000 nm. The pores within the grains and grain boundaries in the ceramic samples act as light scattering centers in transparent ceramics, resulting in a decrease of transmittance [24]. According to the Rayleigh's equation, the scattering intensity increases with decreasing wavelength [25]. The optical transmittance is 0.62 %, 1.68 % and 1.41 % for the Y_2O_3:Er ceramics samples doped with 2 mol%, 5 mol% and 10 mol% $La(OH)_3$, respectively. The transmittance of the specimen doped with 5 mol% $La(OH)_3$ is the best of all in the region from 400 nm to 1100 nm, which is consistent with the microstructure analysis result based on the SEM micrographs of the fracture surface of the Y_2O_3:Er ceramics as shown in Fig. 3. The result indicates that the optimum addition of 5 mol% $La(OH)_3$ helps to improve the optical properties of Y_2O_3:Er ceramics.

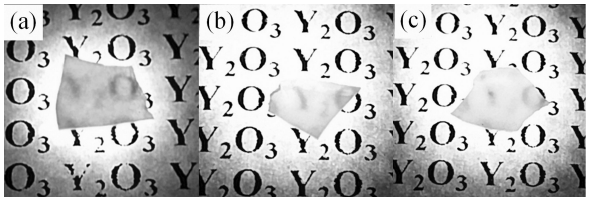

Fig. 5. Photographs of the unpolished Y_2O_3:Er ceramics doped with (a) 2 mol% $La(OH)_3$, (b) 5 mol% $La(OH)_3$, (c) 10 mol% $La(OH)_3$.

Fig. 7 shows the upconversion (UC) emission spectra of the Y_2O_3:0.1%Er^{3+} ceramics samples doped with different doping concentration of $La(OH)_3$ additive under 980 nm LD excitation. The green UC emission bands at 520 – 565 nm and red emission bands at 647 – 667 nm were obtained

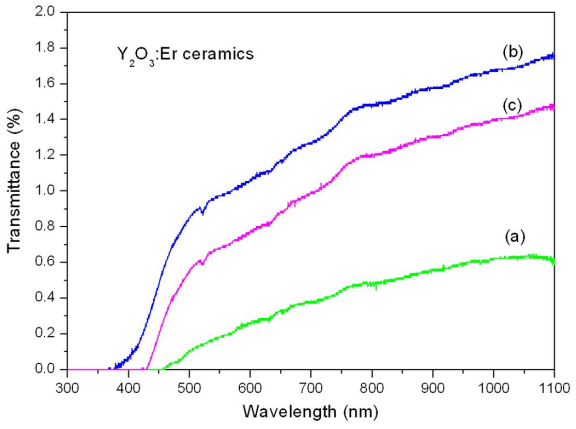

Fig. 6. Optical transmittance spectra of the unpolished Y_2O_3:Er ceramics doped with (a) 2 mol% $La(OH)_3$, (b) 5 mol% $La(OH)_3$, (c) 10 mol% $La(OH)_3$.

for all ceramics samples as shown in Fig. 7a to Fig. 7c, which are ascribed to the radiative transitions of $^2H_{11/2}/^4S_{3/2} \rightarrow {}^4I_{15/2}$ and $^4F_{9/2} \rightarrow {}^4I_{15/2}$ of Er^{3+} ions, respectively [26–28]. In addition, the UC emission intensity increased first and then decreased with the amount of $La(OH)_3$ additive from 2 mol% to 10 mol%. Under relatively weak 980 nm LD excitation, bright green UC luminescence from Er^{3+} doped Y_2O_3 ceramics doped with 2 mol% $La(OH)_3$ can be clearly observed with naked eyes as shown in Fig. 7d, which indicates that high UC emission efficiency can be obtained in the as-fabricated Y_2O_3:Er ceramics.

The UC mechanism of Er^{3+} ions doped materials has been extensively studied and it is known that the excited state absorption process (ESA) as shown in Fig. 8 is the dominant UC mechanism for low doping concentration of Er^{3+} ions [26–28]. Firstly, the Er^{3+} ions at the ground-state $^4I_{15/2}$ are excited to the $^4I_{11/2}$ state by absorbing one 980 nm photon. Following this process, the $^4I_{11/2}$ state relaxes to the $^4I_{13/2}$ state through multiphonon nonradiative relaxation, thus giving rise to the population of the $^4I_{13/2}$ state. Secondly, the Er^{3+} ion located on the $^4I_{11/2}$ level can be further excited to the $^4F_{7/2}$ level through excited-state absorption (ESA) process. Then, nonradiative relaxations could populate the $^2H_{11/2}$ and $^4S_{3/2}$ states, which produces green upconversion emission. In the meantime, the

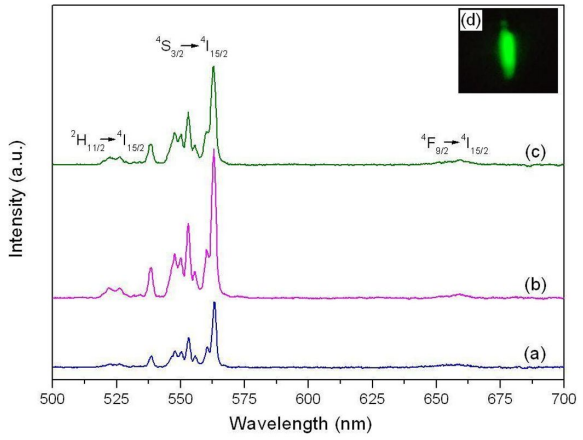

Fig. 7. Upconversion emission spectra of the Y_2O_3:Er ceramics doped with (a) 2 mol% $La(OH)_3$, (b) 5 mol% $La(OH)_3$, (c) 10 mol% $La(OH)_3$ under 980 nm diode laser excitation.

$^4F_{9/2}$ state can be populated by another ESA process from $^4I_{13/2}$ to $^4F_{9/2}$ level of Er^{3+} ions, and the multi-phonon nanoradiative relaxation from $^2H_{11/2}$/$^4S_{3/2}$ to $^4F_{9/2}$ level. And then, the red upconversion emission is observed.

4. Conclusion

Y_2O_3:Er translucent ceramics were fabricated by sintering method using synthetic YOF:Er nanopowders with $La(OH)_3$ as sintering additive. The results showed that a small amount of $La(OH)_3$ helps to control abnormal grain growth, eliminate pores, and increase the optical transmittance of the ceramics samples. Fewer pores in microstructures and better transmittance were obtained with the optimum addition (5 mol%) of $La(OH)_3$. Under 980 nm LD excitation, bright visible upconversion luminescence in all the Y_2O_3:Er ceramics samples was observed, and the UC emission intensity increased first and then decreased with the amount of $La(OH)_3$ additive from 2 mol% to 10 mol%.

Acknowledgements

The work was supported by the NSFC (Grant No. 51062008, 21463014), Key Project of Chinese Ministry of Education (Grant No. 212095), Ground Project of Sci & Tech of Jiangxi (Grant No. KJLD12095).

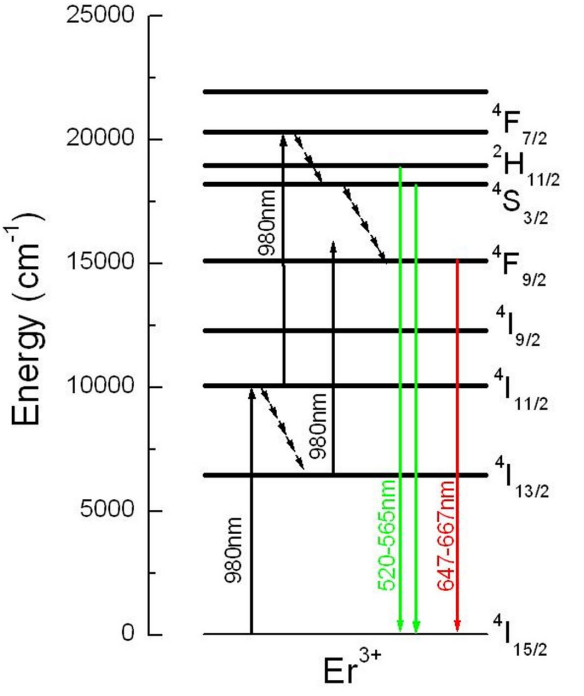

Fig. 8. Upconversion mechanism of Y_2O_3:Er ceramics under 980 nm diode laser excitation.

References

[1] Hoskins R.H., Soffer B.H., *Appl. Phys. Lett.*, 4 (1964) 22.
[2] Alberto U., Camasciali M. M., *J. Alloys Compd.*, 454 (2008) 374.
[3] Huang D.D., Yang Q.H., Wang Y.G., Zhang H.J., *Adv. Mater. Res.*, 299–300 (2011) 641.
[4] Zhu J.F., Wang Z.H., Wang Q., Zhang Z.G., Yang Q.H., Yang J.H., Ma Y.F., Wei Z.Y., *Chin. Opt. Lett.*, 10 (2012) 121403.
[5] Yang Q.H., Lu S.Z., Zhang B., Zhang H.J., Zhou J., Yuan Z.J., Qi Y.F., Lou Q.H., *Opt. Mater.*, 33 (2011) 692.
[6] Zhang H.J., Yang Q.H., Lu S.Z., Huang D.D., Wang Y.G., Wei Z.Y., Wang Q., Zhang Y.D., *Opt. Mater.*, 35 (2013) 766.
[7] Payne S.A., Chase L.L., Smith L.K., Kway W.L., KRUPKE W.F., *IEEE J. Quant. Electron.*, 28 (2002) 2619.
[8] Schweitzer T., Jensen T., Heumann E., Huber G., *Opt.Commun.*, 118 (1995) 557.
[9] Boulanger P.L., Doualan J.L., Girad S., Margerie J., Moncorge R., *Phys. Rev. B*, 60 (1999) 11380.
[10] Pollnau M., Gamelin D.R., Luthi S.R., Gudel H.U., Hehlen M.P., *Phys. Rev. B*, 61 (2001) 3337.
[11] Guan Y., Wei Z.H., Huang Y.L., Maalej R., Jinseo H., *Ceram. Int.*, 39 (2013) 7023.

[12] CAPOBIANCO J.A., BOYER J.C., VETRONE F., SPEGHINI A., BETTINELLI M., *Chem. Mater.*, 14 (2002) 2915.
[13] PARK S., YANG W., PARK C.Y., NOH M., CHOI S., PARK D., JANG H.S., CHO S., *Mater. Res. Bull.*, 71 (2015) 25.
[14] PARK S., *J. Lumin.*, 166 (2015) 176.
[15] YANG R.Y., QIN G.S., ZHAO D., ZHENG K.Z., QIN W.P., *J. Fluor. Chem.*, 140 (2012) 38.
[16] WANG J.L., LIN J.M., WU J.H., HUANG M.L., LAN Z., CHEN Y., TANG S., FAN L.Q., HUANG Y.F., *Electrochim. Acta*, 70 (2012) 131.
[17] RAKOV N., MACIEL G.S., *Opt. Mater.*, 35 (2013) 2372.
[18] DING M.Y., LU C.H., CAO L.H., NI Y.R., XU Z.Z., *Opt. Mater.*, 35 (2013) 1283.
[19] MARTINEZ-CASTRO E., GARCIA-SEVILLANO J., CUSSO F., OCANA M., *J. Alloys Compd.*, 619 (2015) 44.
[20] GRZYB T., WECLAWIAK M., ROZOWSKA J., LIS S., *J. Alloys Compd.*, 576 (2013) 345.
[21] GRZYB T., WECLAWIAK M., PEDZINSKI T., LIS S., *Opt. Mater.*, 35 (2013) 2226.
[22] GUO Y.Y., WANG D.Y., WU X.H., WANG Q.K., HE Y., *J. Alloys Compd.*, 688 (2016) 816.
[23] LI X.K., MAO X.J., FENG M.H., QI S., JIANG B.X., ZHANG L., *J. Eur. Ceram. Soc.*, 36 (2016) 2549.
[24] PEELEN J.G.J., METSELAA R., *J. Appl. Phys.*, 45 (1974) 216.
[25] IKESUE A., KAMATA K., YAMAMOTO T., YAMAGA I., *J. Am. Ceram. Soc.*, 80 (1997) 1517.
[26] GUO Y.Y., WANG D.Y., WANG F., *Opt. Mater.*, 42 (2015) 390.
[27] ZHANG J., WANG S.W., AN L.Q., LIU M., CHEN L.D., *J. Lumin.*, 122-123 (2007) 8.
[28] SHEN X., NIE Q.H., XU T.F., DAI S.X., WANG X.S., *Phys. B*, 381 (2006) 219.

Received 2018-12-01
Accepted 2019-04-23